

A Unifying Action Principle for Classical Mechanical Systems

A. Rothkopf¹ and W. A. Horowitz²

¹*Department of Mathematics and Physics, University of Stavanger,
Kristine Bonnevis vei 22, 4021 Stavanger, Norway*

²*Department of Physics, University of Cape Town,
Private Bag X3, Rondebosch 7701, South Africa*

The modern theory of classical mechanics, developed by Lagrange [1], Hamilton [2] and Noether [3], attempts to cast all of classical motion in the form of an optimization problem, based on an energy functional called the classical action. The most important advantage of this formalism is the ability to manifestly incorporate and exploit symmetries and conservation laws. This reformulation succeeded for unconstrained and holonomic systems that at most obey position equality constraints. Non-holonomic systems, which obey velocity dependent constraints or position inequality constraints, are abundant in nature and of central relevance for science, engineering and industry. All attempts so far to solve non-holonomic dynamics as a classical action optimization problem have failed. Here we utilize the classical limit of a quantum field theory action principle [4–6] to construct a novel classical action for non-holonomic systems. We therefore put to rest the 190 year old question of whether classical mechanics is variational, answering in the affirmative. We illustrate and validate our approach by solving three canonical model problems by direct numerical optimization of our new action. The formalism developed in this work significantly extends the reach of action principles to a large class of relevant mechanical systems, opening new avenues for their analysis and control both analytically and numerically.

I. INTRODUCTION

A mechanical system, subject to one or multiple constraints that are not derivable from position constraint equalities is called non-holonomic [7]. The most common form of non-holonomic constraints are velocity dependent constraints, as well as position inequality constraints. The rolling-spinning disc on an incline [8], as well as a particle under constant gravity in the presence of hard surfaces are two such challenging classic models.

Non-holonomic systems are abundant in the field of robotics and autonomous transport (see e.g. [9]). Besides reliable prediction of system motion for given initial conditions (forward kinematics) inference of admissible initial data and necessary external forces to achieve a certain final state (inverse kinematics and control) is sought after (see e.g. [10]). Non-holonomic dynamics furthermore arise in the description of contact forces [11–13] among macroscopic materials, relevant in mineral and crop processing. In the absence of an action principle for non-holonomic systems, the analysis of these systems is limited to the explicit study of forces and cannot benefit from the powerful simplifications and tools offered by a purely energy based variational treatment available to holonomic systems (see e.g. [14]).

Hamilton showed that mechanical systems with conservative forces are variational (for a textbook see [15]). I.e. there exists an action (cost) functional $S = \int dt L[\mathbf{q}, \dot{\mathbf{q}}]$, constructed from the system Lagrangian L (a measure of energy), whose critical point $\mathbf{q}(t)_{\text{cl}} \in \mathbb{R}^d$, given boundary data $\mathbf{q}(t_i)_{\text{cl}}, \mathbf{q}(t_f)_{\text{cl}}$, encodes the classical trajectory of the system via the following stationarity condition

$$\delta S = 0, \quad \Leftrightarrow \quad \frac{d}{dt} \left(\frac{\partial L}{\partial \dot{q}^i} \right) - \frac{\partial L}{\partial q^i} = 0. \quad (1)$$

The condition on the left yields the same trajectory as the Euler-Lagrange equations of motion on the right, which are equivalent to Newton's second law. Note that at this point we have made a subtle change from a boundary value problem (left) to an initial value problem (right).

The variational formulation of classical mechanics puts symmetries center stage, since the Lagrangian transforms as a scalar under space-time and internal symmetries. Conceptually the variational formulation forms the basis for Noether's celebrated theorem [3], connecting symmetries and conserved charges, and in practice allows for the development of reliable numerical solvers, such as Finite Element Ritz-Galerkin methods (see e.g. [16, 17]).

Constraints represent the elegant implementation of (idealized) forces \mathbf{F}_C , acting on or within a mechanical system. Equality constraints are concisely described by constraint functions $\mathbf{g}(\mathbf{q}, \dot{\mathbf{q}}) \in \mathbb{R}^{n \leq d}$ as $g^a(\mathbf{q}, \dot{\mathbf{q}}) = 0$. Expressed as forces, constraints fall into the purview of Newton's second law. And while the application of Newton's equation of motion will yield the correct trajectory, determining the forces explicitly may prove infeasible in practice and one loses the advantages of an action formulation, such as e.g. first integrals of motion [15].

Holonomic constraints, which only depend on position, $g^a(\mathbf{q}) = 0$ can be incorporated into Hamilton's action principle eq. (1) by adjoining the constraint functions to the Lagrangian via Lagrange multiplier functions $\lambda(t) \in \mathbb{R}^n$. The action then reads $S = \int dt (L[\mathbf{q}, \dot{\mathbf{q}}] + \lambda^a g^a(\mathbf{q}))$ and one treats the multipliers as independent degrees of freedom on the same footing as the generalized coordinates \mathbf{q} . Adjoining general non-holonomic constraints $g^a(\mathbf{q}, \dot{\mathbf{q}}) = 0$ fails to produce the correct classical trajectory [18], since the velocity dependent restrictions on the variations of the path are not implemented consistently via eq. (1).

Prior to this work, non-holonomic constrained systems could only be treated on the level of their equations of motion. According to the Lagrange-d'Alembert principle (see [18] for a detailed derivation), which requires the constraint forces do no virtual work $F_C^i \delta q^i = 0$, one may adjoin the equations of motion of the unconstrained system via Lagrange multipliers

$$\frac{d}{dt} \left(\frac{\partial L}{\partial \dot{q}^i} \right) - \frac{\partial L}{\partial q^i} = \lambda^a \frac{\partial g^a}{\partial \dot{q}^i}. \quad (2)$$

The non-trivial $\dot{\mathbf{q}}$ derivative in the λ dependent term arises from the need to consider only variations consistent with the constraints and can be derived via Gauss' principle [18, 19]. Note that solving eq. (2) may lead to $\lambda(t)$'s that are non-smooth while the physical trajectories remain smooth. Equation (2) goes beyond the conventional Dirac [20] and Gotay-Nester [21] algorithms, which fail for non-integrable semi-holonomic constraints. For their recent non-holonomic generalization via the Flannery bracket see [22]. A redefinition of velocities, motivated by the path integral (see, e.g., [23]) fails when velocities enter quadratically in the constraint. Equation (2) covers holonomic constraints, which by time differentiation turn into linear velocity constraints $\frac{d}{dt} g^a = \frac{\partial g^a}{\partial \dot{q}^i} \dot{q}^i$. Information about absolute values encoded in the original holonomic constraint are provided by initial conditions. Hamilton's variational principle is unable to yield eq. (2), as shown in detail in Ref. [18].

Inequality position constraints $g^a(\mathbf{q}) \leq 0$ present different challenges, since the idealized normal (contact) forces they encode can lead to non-smooth trajectories (see, e.g., the discussion in [24]). In practice, such systems are treated by following the unconstrained equations of motion in the interior of the allowed domain and manually identifying the jumps in the canonical momenta at the boundary (within the normal cone), implemented under an energy conservation constraint. A causal action principle intrinsically maintains conservation laws and in addition would provide access to the trajectory globally, rendering superfluous the need to manually identify points of contact. Normal forces are closely related to sliding friction forces, such as in Coulomb friction [25], which is abundant in realistic mechanical systems, and cannot be captured by either the Lagrange-d'Alembert nor Hamilton's principle.

In this work we take inspiration from an action principle originally developed in the context of quantum theory and heuristically construct from its classical limit an action for non-holonomic systems. For general velocity dependent constraints this action principle reproduces the correct Lagrange-d'Alembert equations of motion eq. (2) at its critical point. We also show how our new action principle can be used to approximate both the non-smooth dynamics from inequality constraints and that of sliding friction on hard surfaces. In case of non-smooth trajectories our approach automatically identifies and incorporates the points of impact along the trajectory.

II. ACTION PRINCIPLE FOR NON-HOLONOMIC SYSTEMS

The need for a more general action principle beyond Hamilton is evident from the fact that in contrast to Newton's second law, eq. (1) cannot capture dissipative systems with velocity dependent forces (see, e.g., [15]) nor velocity dependent non-holonomic constraints (see [18]). First and foremost however, Hamilton's principle is unable to capture the causal dynamics of initial value problems to start with. Indeed the need to provide boundary data $\mathbf{q}(t_f)_{cl}$ at final time prevents the direct application of $\delta S = 0$ to determine particle motion.

In quantum field theory it has long been known how to treat initial value problems variationally on the level of the system action via the Schwinger-Keldysh [4] (or Kadanov-Baym [5]) in-in formalism, which relies on a doubling of the degrees of freedom. In [6] Galley rediscovered the classical limit of the in-in formalism independently and understood it as a double shooting method.

After a brief introduction to this action principle for initial value problems, we show how to amend it by constraint functions via Lagrange multipliers, in order to recover the correct equation of motion eq. (2) for general velocity dependent constraints. Subsequently we use the versatility of the approach to implement the explicit constraint normal forces underlying inequality position constraints and sliding friction forces.

Action principle for initial value problems Hamilton's principle requires specification of acausal data $\mathbf{q}(t_f)_{cl}$ to avoid boundary terms. As described in detail in [6], classical Schwinger-Keldysh instead avoids these terms by introducing a set of doubled degrees of freedom $\mathbf{q}_1, \dot{\mathbf{q}}_1$ on the so-called forward time branch and $\mathbf{q}_2, \dot{\mathbf{q}}_2$ on the backward branch. The most general action can be written as

$$S_{SK} = \int dt L[\mathbf{q}_1, \dot{\mathbf{q}}_1] - L[\mathbf{q}_2, \dot{\mathbf{q}}_2] + \Lambda[\mathbf{q}_1, \dot{\mathbf{q}}_2, \mathbf{q}_2, \dot{\mathbf{q}}_2]. \quad (3)$$

For systems with conservative forces $\Lambda = 0$, while for dissipative systems in general the action does not decompose into individual Lagrangians on each branch and $\Lambda \neq 0$ takes on the role of a classical Feynman-Vernon influence functional [26].

The variational principle is most lucidly stated after introducing the transformed coordinates $\mathbf{q}_+ = (\mathbf{q}_1 + \mathbf{q}_2)/2$ and $\mathbf{q}_- = (\mathbf{q}_1 - \mathbf{q}_2)$ ¹ and reads

$$\delta S_{SK}|_{\mathbf{q}_- = 0} = 0 \quad \Leftrightarrow \quad \left. \frac{\delta S_{SK}}{\delta \dot{q}_-^i} \right|_{\mathbf{q}_- = 0, \mathbf{q}_+ = \mathbf{q}_{cl}} = 0. \quad (4)$$

¹ In the quantum Schwinger-Keldysh approach, $\mathbf{q}_+, \mathbf{q}_-$ are also known as the classical and quantum degrees of freedom, respectively.

Note that by enforcing the so-called *physical limit* $\mathbf{q}_- = 0$ after variation, the artificial doubling of the degrees of freedom is undone and we remain with the correct equations of motion for the classical trajectory $\mathbf{q}_+ = \mathbf{q}_{\text{cl}}$. In order to avoid acausal boundary terms we need to specify besides initial data also so-called connecting conditions

$$\underbrace{\mathbf{q}_+(t_i) = \mathbf{q}_{\text{cl}}(t_i),}_{\text{init. cond.}} \quad \underbrace{\mathbf{q}_-(t_f) = 0,}_{\text{conn. cond.}} \quad (5)$$

$$\underbrace{\dot{\mathbf{q}}_+(t_i) = \dot{\mathbf{q}}_{\text{cl}}(t_i),}_{\text{init. cond.}} \quad \underbrace{\dot{\mathbf{q}}_-(t_f) = 0.}_{\text{conn. cond.}}$$

It is important to note that this action principle allows us to implement general forces $\mathbf{F}(\mathbf{q}, \dot{\mathbf{q}})$ via interaction terms of the form $\Lambda = F^i(\mathbf{q}_+, \dot{\mathbf{q}}_+) q_-^i$. One may thus also include dissipative, velocity dependent forces [6]. I.e. if an explicit form of the forces acting in a system is known, their effect can hence be straightforwardly incorporated in S_{SK} . In the subsequent section we show how to also incorporate implicitly defined constraint forces.

General velocity constraints Without loss of generality and for the sake of notational clarity let us focus on non-dissipative systems $\Lambda = 0$. Our goal is to reproduce the Lagrange-d'Alembert equations of motion in eq. (2) in the presence of general velocity dependent constraints described by the n functions $g^a(\mathbf{q}, \dot{\mathbf{q}}) = 0$. When introducing correspondingly n Lagrange multiplier functions λ it is important to recognize that one elevates the constraint equations to additional equations of motion of the system. Furthermore, the formalism asks us to consider two copies λ_1 and λ_2 as dynamical degrees of freedom. I.e. we must add to the classical Schwinger-Keldysh action terms that not only reproduce eq. (2) but that also determine the values of λ_{cl} . This can be achieved via

$$S_{\text{cSK}} \equiv \int dt L[\mathbf{q}_1, \dot{\mathbf{q}}_1] - L[\mathbf{q}_2, \dot{\mathbf{q}}_2] \quad (6)$$

$$+ \lambda_-^a g^a(\mathbf{q}_+, \dot{\mathbf{q}}_+) - \lambda_+^a q_-^i \left. \frac{\partial g^a}{\partial \dot{q}^i} \right|_{\mathbf{q}=\mathbf{q}_+}.$$

By applying (4) to eq. (6) one confirms that the λ_-^a term establishes the meaning of the Lagrange multipliers as enforcing the constraint, while the λ_+^a term provides the correct constraint force contributions in eq. (2).

Position inequality constraints Position inequality constraints $g^a(\mathbf{q}) \leq 0$ implicitly define idealized potential barriers of sufficient height, at which the propagating degrees of freedom reflect. The reversal of the momentum of the particle normal to the surface appears to happen instantaneously, leading to non-smooth trajectories. We may model such behavior explicitly with simple step functions as potentials $V^a(\mathbf{q}) = \Theta(g^a(\mathbf{q}))$, whose arguments prescribe the accessible domain. The associated normal forces \mathbf{F}_N^a given by $(\mathbf{F}_N^a)_i = -\delta(g^a(\mathbf{q})) \frac{\partial g^a}{\partial q^i}$ are represented by a Dirac delta impulse occurring at the instant that the system makes contact with the boundary of the allowed domain.

Sliding friction forces $\mathbf{F}_R^a = \mu^a |\mathbf{F}_N^a| (-\dot{\mathbf{q}}_{\parallel} / |\dot{\mathbf{q}}_{\parallel}|)$ associated with normal forces \mathbf{F}_N^a via the respective coefficient

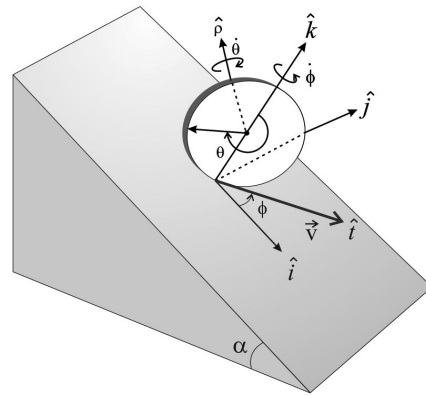


FIG. 1. **Sketch of the rolling-spinning disk on an incline.** x, y encode the center of mass $\mathbf{r}_{\text{c.m.}} = x\hat{i} + y\hat{j} + z\hat{k}$ and the angles θ, ϕ encode rolling and spinning motion. Reprinted from [8], with the permission of AIP Publishing.

of kinetic friction μ^a , on the other hand, oppose motion and thus acquire a dependence on velocity along the contact surface.

In the classical Schwinger-Keldysh approach we can incorporate the physics of contact and sliding friction directly on the level of a generalized interaction term as

$$S_{\text{iSK}} = \int dt L[\mathbf{q}_1, \dot{\mathbf{q}}_1] - L[\mathbf{q}_2, \dot{\mathbf{q}}_2] \quad (7)$$

$$+ q_-^i \sum_a (\mathbf{F}_N^a)_i \Big|_{\mathbf{q}=\mathbf{q}_+} + q_-^i \sum_a \mu^a |\mathbf{F}_N^a| \frac{-\dot{q}_{\parallel}^i}{|\dot{\mathbf{q}}_{\parallel}|} \Big|_{\mathbf{q}=\mathbf{q}_+},$$

where $\dot{\mathbf{q}}_{\parallel}$ denotes the projection of the velocity parallel to the contact surface.

Note that the normal force term does not depend on the velocities $\dot{\mathbf{q}}$ and thus does not affect the invariance of the action under time translations, guaranteeing the preservation of energy by construction. While the constraint potential $V^a(\mathbf{q})$ could be included in Hamilton's principle, only the classical Schwinger-Keldysh approach allows one to formulate this physical setup as an initial value problem. The sliding friction force does depend on velocity, exposing its dissipative character.

Since contact is not actually instantaneous in nature, we may safely regularize the associated normal force. We implement the contact force here via a generalized interaction term and subsequently regularize the the delta impulse by a Gaussian with a width σ . This width σ is chosen small enough to appear localized within the desired level of accuracy.

III. APPLICATION TO MODEL SYSTEMS

Non-holonomic velocity constraints Our first application is the rolling-spinning disk [8] with radius R and mass M on an incline of angle α in the presence of constant gravity g , sketched in fig. 1. The system is described

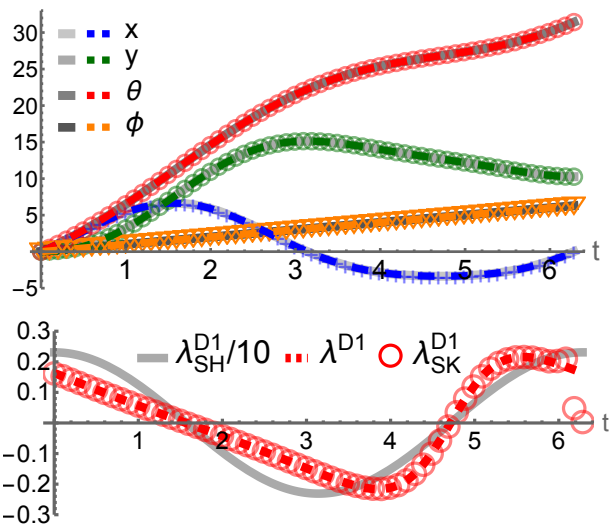


FIG. 2. **Time evolution of a rolling-spinning disc.** Motion obtained via the semi-holonomic (solid gray) and non-holonomic (dashed color) Lagrange-d'Alembert equations of motion as well as via the critical point of our novel classical SK action eq. (A1) (color symbols). Physical degrees of freedom in top-, the Lagrange multiplier to g^{D1} in the bottom panel. λ_{SK}^{D1} close to t_f shows effect of imposing connecting conditions with ξ_λ^{D2} .

by four interdependent degrees of freedom x, y, θ and ϕ . The former two encode the position of the center of mass $\mathbf{r}_{c.m.} = x\hat{i} + y\hat{j} + z\hat{k}$, while the latter two angles θ, ϕ encode the rolling and spinning motion. Given the moment of inertia I_S about the symmetry axis and I_D about the fixed spinning axis, the Lagrangian reads

$$L_D = \frac{1}{2}M(\dot{x}^2 + \dot{y}^2) + \frac{1}{2}I_S\dot{\theta}^2 + \frac{1}{2}I_D\dot{\phi}^2 + Mgx\sin(\alpha). \quad (8)$$

For non-slip motion, we ensure $g_{D1} = \dot{x}^2 + \dot{y}^2 - R^2\dot{\theta}^2 = 0$ and $g_{D2} = \dot{x}\sin(\phi) - \dot{y}\cos(\phi) = 0$. Both constraints are non-integrable but captured by the Lagrange-d'Alembert principle of eq. (2).

With the help of g_{D2} , one can turn g_{D1} into semi-holonomic form [8], for which we solve eq. (2) using the `Mathematica` `NDSolve` command [27]. We plot these results² as gray solid lines in fig. 2. Physical trajectories are shown in the top panel and the Lagrange multiplier λ_{SH}^{D1} associated with the linearized semi-holonomic g_{D1} in the bottom panel. If we instead solve eq. (2) with the non-linear g_{D1} we obtain the colored dashed lines. Note that the same physical trajectories are obtained, while λ^{D1} , now enforcing a another constraint, differs³.

² All results shown in fig. 2 use $g = 9.8 \text{ m/s}^2$, $\alpha = \pi/6$, $M = 1 \text{ kg}$, $R = 1 \text{ m}$, $I_S = 1/2 \text{ kg m}^2$ and $I_D = 1/4 \text{ kg m}^2$, as well as initial values $x_i = 0 \text{ m}$, $\dot{x}_i = 5 \text{ m/s}$, $y_i = 0 \text{ m}$, $\dot{y}_i = 0 \text{ m/s}$, $\theta_i = 0$, $\dot{\theta}_i = 5 \text{ rad/s}$, $\phi_i = 0$, $\dot{\phi}_i = 1 \text{ rad/s}$.

³ A reference implementation of both numerical examples is available at [28]

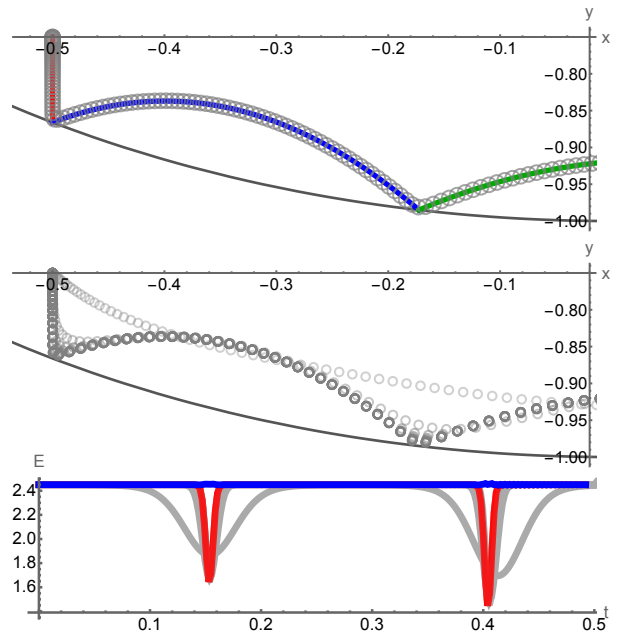


FIG. 3. **Point mass falling in a tumbler.** (Top) Motion obtained via Newton's 2nd law (solid colors) and from the critical point of our SBP424 discretized action (gray circles) with $N = 256$ and $\sigma = 1/110$. (Center) Convergence of the critical point towards the correct solution as the width of the Gaussian $\sigma = 1/10 \dots 1/110 \text{ m}$ is decreased (light to dark gray). (Bottom) Total energy E is shown as blue solid curve. Its kinetic and gravitational contribution are given in red. The gray lines show the change in kinetic and gravitational contributions as σ is reduced.

Using eq. (8) with the non-linear g_{D1} and g_{D2} in eq. (6), introducing $\lambda_{1,2}^{D1}$ and $\lambda_{1,2}^{D2}$ Lagrange multiplier functions to encode the two constraints, one obtains the corresponding classical Schwinger-Keldysh action.

To numerically determine the trajectory we evaluate the critical point of this action after discretization, following [29]. We rely on summation-by-parts (SBP) finite difference operators (for reviews see [30–32]), which mimic integration-by-parts (IBP) exactly in the discrete setting and deploy a time grid with N steps $\Delta t = (t_f - t_i)/(N - 1)$. Details of the discretization procedure and the explicit form of the numerical action is provided in appendix A 1.

Choosing a fourth order accurate SBP discretization SBP242 on $N = 64$ points to span the time interval $t_f - t_i = 2\pi \text{ s}$, we carry out a numerical optimization with the `IPOTP` library accessible through the `FindMinimum` command of `Mathematica` to obtain the critical point of the discretized action eq. (A1). The result is plotted as colored symbols in fig. 2 and shows excellent agreement with the solution of eq. (2) given as dashed colored lines.

Position inequality constraints Our second application is the particle under constant gravity in a hard-walled tumbler in the absence of friction. The Lagrangian

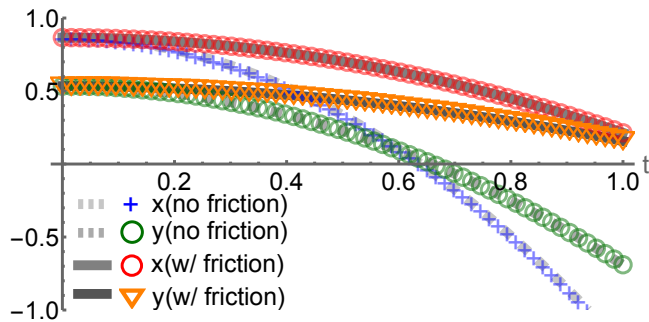


FIG. 4. **Sliding motion along an incline of angle $\alpha = \pi/6$ in constant gravity.** Trajectories from Newton’s second law in gray in the absence (dashed) and presence (solid) of kinetic Coulomb friction $\mu = 4/10$. Trajectories from the critical point of action eq. (A4) are given as open colored symbols, where the normal force is regularized with $\sigma = 1/70\text{m}$ and initial position is offset by $\delta = 1/30\text{m}$.

of the unconstrained system is

$$L_S = \frac{1}{2}m(\dot{x}^2 + \dot{y}^2) - mgy. \quad (9)$$

The accessible regime is given by $g_S = x^2 + y^2 - R^2 \leq 0$, which we implement by the step function potential $V(x, y) = V_0\Theta(g_S)$. We regulate the resulting delta impulse force on the boundary in eq. (7) using a Gaussian of width σ , which leads us to $\mathbf{F}_N(\mathbf{r}) = -\frac{V_0}{\sqrt{2\pi\sigma^2}}e^{-(x^2+y^2-R^2)/2\sigma^2}\mathbf{r}$ where $\mathbf{r} = (x, y)$. In order for the particle to be reflected we must choose V_0 larger than the largest possible kinetic energy the particle may acquire, provided by the conserved initial energy of the system.

Being a system that can produce non-smooth trajectories, we set out to solve it numerically, directly from the critical point of the SBP discretized action, whose explicit expression is provided in appendix A 2.

Note that a large $\sigma/R \sim 1$ corresponds to a fuzzy boundary and only by reducing its value will one approach the hard wall limit. One can determine self-consistently smallest admissible choice of σ for a given time resolution by monitoring the mechanical energy $E = \frac{1}{2}M((dx/dt)^2 + (dy/dt)^2) + Mgy$. The discretized energy is given explicitly in appendix A 2. As the Gaussian impulse becomes too sharp to be resolved, the energy after impact with the wall will show oscillatory artifacts around its well preserved value.

In the top panel of fig. 3 we show our numerical result for the critical point of eq. (A2), discretized with the fourth order accurate SBP424 scheme, obtained via the IPOTP method of `Mathematica`’s `FindMinimum` command. The gray open symbols correspond to a point mass with $M = 1$ kg in a tumbler of radius $R = 1$ m, positioned initially at rest at $x_i = -1/2$ m, $y_i = -3/4$ m. The time interval is discretized with $N = 256$ steps of size $\Delta t = \frac{1}{2(N-1)}$ s and the delta impulse with $V_0 = 10$ J

regulated with a width parameter $\sigma = 1/110$ m. We find excellent agreement with the manually computed trajectory according to Newton’s second law, shown as solid colored lines. Note that in the action based approach we did not have to locate the points of impact manually, as the method automatically generates the complete global trajectory of the particle.

In the center panel of fig. 3 we show that our solution systematically approaches the non-smooth trajectory for the hard-wall tumbler, as the parameter σ is reduced from $1/10$ m to $1/110$ m. The reason we stop at $\sigma = 1/110$ m follows from an analysis of the total energy in the bottom panel shown as blue line. Upon magnification, an inspection by eye reveals that the energy begins to exhibit small oscillatory artifacts close to $t = 1/2$ s after the second impact. We have checked that increasing N and decreasing Δt allows us to further reduce σ . The red curve in the bottom panel denotes the mechanical energy E without the contributions from the boundary. The regularized delta impulse with $\sigma = 1/110$ m temporarily changes the kinetic energy of the particle, but returns it to the same total mechanical energy as before the impact. The gray lines illustrate the different changes in mechanical energy for larger values of the σ parameter.

As a final example, we demonstrate how one can incorporate normal and friction forces in our action approach. Consider the motion of a point particle mass sliding down an inclined plane of angle $\alpha = \pi/6$ whose surface has a non-zero coefficient of kinetic friction μ . Since the mass cannot penetrate the surface of the incline, we have an inequality constraint $x \tan \alpha - y \geq 0$ that we treat in addition to the standard Lagrangian eq. (9). Let us introduce the normal force, regularized by a Gaussian with width σ , which reads $\mathbf{F}_N = -\frac{V_0}{\sqrt{2\pi\sigma^2}}e^{-(x \tan \alpha - y)^2/2\sigma^2}(\tan \alpha \hat{x} - \hat{y})$. The kinetic friction force then reads $\mathbf{F}_R = \mu \frac{V_0}{\sqrt{2\pi\sigma^2}}e^{-(x \tan \alpha - y)^2/2\sigma^2}(\hat{x} + \tan \alpha \hat{y})$. Note that due to the regularization with σ , we also must offset the sliding mass point away from the exact position of the hard surface it moves along by a distance δ . As the regularization σ of the normal force is diminished with increasing number of grid points N , similar to the previous example, the offset δ too may be reduced.

In fig. 4 we present numerical results for motion on the incline from the critical point of the discretized action given explicitly in eq. (A4) and obtained via the IPOTP method of `Mathematica`’s `FindMinimum` command. We have chosen a time interval of $t_f - t_i = 1$ s discretized on $N = 64$ points and deploy the SBP424 discretization scheme. Since the motion in this case is smooth $N = 64$ suffices to achieve result already visually indistinguishable from Newton’s law, where for non-smooth motion $N = 256$ was required. Motion is initialized at $x_i = \cos \alpha$ m and $y_i = (\sin \alpha + \delta)$ m with $\delta = 1/30$ m with the potential barrier set at $V_0 = 5$ J. The offset δ was chosen to minimize residual oscillatory artifacts arising from the

regularization of the normal force with $\sigma = 1/70$ m.

Comparing in fig. 4 to the direct solution of Newton's second law in the absence (gray dashed) and presence (gray solid) of friction we find excellent agreement of the action based results (colored open symbols). We have checked that reducing σ together with δ quantitatively improves the agreement between the two approaches.

IV. CONCLUSION

Prior to this work, the trinity of principles of classical mechanics could be ordered according to their applicability to classes of problems from the broadest, Newton (forces), to Lagrange-d'Alembert (variational equations of motion), to the most restrictive, Hamilton (action).

190 years after Hamilton, we have upended this ordering to place the action-based approach on an equal footing to forces. Our action achieves this upending by exploiting the doubled degrees of freedom of the classical limit of the Schwinger-Keldysh quantum mechanical action principle, allowing one to incorporate implicit forces defined through holonomic and non-holonomic equality and inequality constraints and any explicit generalized force (including friction).

Beyond the re-writing of textbooks that our work will require, our action principle opens up the advantages of an action-based approach to whole new classes of problems with important applications in academia and industry.

ACKNOWLEDGMENTS

A. R. and W. A. H. acknowledge support by the ERASMUS+ project 2023-1-NO01-KA171-HED-000132068. W. A. H. thanks the South African National Research Foundation and the SA-CERN Collaboration for financial support and the BNL EIC theory institute for its hospitality.

AUTHOR CONTRIBUTIONS

Motivated by gauge fixing of coordinate maps [33], A. R. put forward the idea of exploiting the doubled degree of freedom formalism to capture quadratic velocity dependent non-holonomic constraints. A. R. and W. A. H. with equal contribution developed the classical SK formalism for velocity dependent constraints, as well as the formalism to incorporate inequality constraints based on generalized forces. A. R. implemented the formalism for the example systems discussed in this paper, available as supplementary material.

ADDITIONAL INFORMATION

Correspondence and requests for materials should be addressed to Alexander Rothkopf.

Supplementary Information is available for this paper.

The authors declare no competing interests.

-
- [1] Lagrange, J. *Mechanique analytique, chez la veuve de-saint. Paris: Libraire, Rue de Foire St Jacques* (1788).
- [2] Hamilton, W. R. *On a general method in dynamics* (Richard Taylor United Kindom, 1834).
- [3] Noether, E. Invariante variationsprobleme. *Nachr. Akad. Wiss. Göttingen, II* 235–257 (1918).
- [4] Keldysh, L. V. Diagram technique for nonequilibrium processes. In *Selected Papers of Leonid V Keldysh*, 47–55 (World Scientific, 2024).
- [5] Kadanoff, L. P. *Quantum statistical mechanics* (CRC Press, 2018).
- [6] Galley, C. R. Classical Mechanics of Nonconservative Systems. *Phys. Rev. Lett.* **110**, 174301 (2013).
- [7] Bloch, A. M., Marsden, J. E. & Zenkov, D. V. Non-holonomic dynamics. *Notices of the AMS* **52**, 320–329 (2005).
- [8] Flannery, M. R. The enigma of nonholonomic constraints. *American Journal of Physics* **73**, 265–272 (2005).
- [9] Murray, R. M., Li, Z. & Sastry, S. S. *A mathematical introduction to robotic manipulation* (CRC press, 2017).
- [10] Baillieul, J., Bloch, A., Crouch, P. & Marsden, J. *Non-holonomic Mechanics and Control*. Interdisciplinary Applied Mathematics (Springer New York, 2007).
- [11] Hertz, H. Ueber die berührung fester elastischer körper. *Journal für die reine und angewandte Mathematik* **93**, 156–171 (1882).
- [12] Johnson, K. L. *Contact mechanics* (Cambridge university press, 1987).
- [13] Mindlin, R. D. *Compliance of elastic bodies in contact* (American Society of Mechanical Engineers, 1949).
- [14] De Sapio, V., Khatib, O. & Delp, S. Least action principles and their application to constrained and task-level problems in robotics and biomechanics. *Multibody System Dynamics* **19**, 303–322 (2008).
- [15] Goldstein, H. *Classical mechanics* (Pearson Ed., 2011).
- [16] Gander, M. J. & Wanner, G. From euler, ritz, and galerkin to modern computing. *SIAM Review* **54**, 627–666 (2012).
- [17] Thomée, V. *Galerkin finite element methods for parabolic problems*, vol. 25 (Springer, 2007).
- [18] Flannery, M. R. d'Alembert–Lagrange analytical dynamics for nonholonomic systems. *Journal of Mathematical Physics* **52**, 032705 (2011).
- [19] Papastavridis, J. G. *Analytical Mechanics* (World Scientific, 2014).
- [20] Dirac, P. *Lectures on Quantum Mechanics*. Belfer Graduate School of Science (Dover Publications, 2001).
- [21] Gotay, M. J. & Nester, J. M. Presymplectic lagrangian systems. I : the constraint algorithm and the equivalence theorem. *Annales de l'institut Henri Poincaré. Section A, Physique Théorique* **30**, 129–142 (1979).

- [22] Horowitz, W. A. & Rothkopf, A. Even more generalized hamiltonian dynamics (2024). URL <https://arxiv.org/abs/2408.14420>. 2408.14420.
- [23] Jackiw, R. (Constrained) quantization without tears. In *2nd Workshop on Constraint Theory and Quantization Methods*, 367–381 (1993).
- [24] Fetecau, R. C., Marsden, J. E., Ortiz, M. & West, M. Nonsmooth lagrangian mechanics and variational collision integrators. *SIAM J. on Applied Dynamical Systems* **2**, 381–416 (2003).
- [25] Coulomb, C. Sur une application des regies de maximis et minimis a quelques problemes de statique, relatifs a l’architecture. *Memoires deMathematique et de Physique, Academic Royal des Sciences, par diversSavans, Flannel* (1773).
- [26] Feynman, R. & Vernon, F. The theory of a general quantum system interacting with a linear dissipative system. *Annals of Physics* **24**, 118–173 (1963).
- [27] Inc., W. R. Mathematica v.13.2. URL <https://www.wolfram.com/mathematica>. Champaign, IL, 2024.
- [28] Rothkopf, A. Accompanying Mathematica Notebooks for “A Unifying Action Principle for Classical Mechanical Systems” (2024). URL <https://doi.org/10.5281/zenodo.13771168>.
- [29] Rothkopf, A. & Nordström, J. A new variational discretization technique for initial value problems bypassing governing equations. *J. Comput. Phys.* **477**, 111942 (2023). 2205.14028.
- [30] Svård, M. & Nordström, J. Review of summation-by-parts schemes for initial–boundary–value problems. *Journal of Computational Physics* **268**, 17–38 (2014).
- [31] Fernández, D. C. D. R., Hicken, J. E. & Zingg, D. W. Review of summation-by-parts operators with simultaneous approximation terms for the numerical solution of partial differential equations. *Computers & Fluids* **95**, 171–196 (2014).
- [32] Lundquist, T. & Nordström, J. The SBP-SAT technique for initial value problems. *Journal of Computational Physics* **270**, 86–104 (2014).
- [33] Rothkopf, A., Horowitz, W. A. & Nordström, J. Exact symmetry conservation and automatic mesh refinement in discrete initial boundary value problems (2024). URL <https://arxiv.org/abs/2404.18676>. 2404.18676.

Appendix A: Methods

1. Discretized action for the rolling-falling disk

Given a time grid with N steps $\Delta t = (t_f - t_i)/(N - 1)$, the physical degrees of freedom of the rolling-falling disk are represented by N -component arrays $\mathbf{x}_{1,2}$, $\mathbf{y}_{1,2}$, $\boldsymbol{\theta}_{1,2}$ and $\boldsymbol{\phi}_{1,2}$. Integration by parts connects integration and differentiation, hence we must choose a compatible quadrature matrix \mathbb{H} implementing $\int dt f(t)g(t) \approx \mathbf{f}^T \mathbb{H} \mathbf{g}$ and finite difference operators $\mathbb{D} = \mathbb{H}^{-1} \mathbb{Q}$. Here the matrix \mathbb{Q} encodes the finite difference stencil structure and ensures the SBP property via $\mathbb{Q}^T + \mathbb{Q} = \text{diag}[-1, 0, \dots, 0, 1]$. The lowest order diagonal SBP121 approach combines the trapezoid rule $\mathbb{H} = \Delta t \text{diag}[\frac{1}{2}, 1, \dots, 1, \frac{1}{2}]$ with the lowest order central symmetric finite difference stencil in the interior, and the forward and backward stencils on the backward and forward boundary respectively (for details and explicit expression for the higher order SBP242 see [29]). In a numerical setting the initial conditions and connecting conditions of eq. (5) must be included explicitly on the action level, which we accomplish by adding additional Lagrange multiplier variables, κ for initial and ξ for connecting conditions, to the action functional eq. (6)⁴. The explicit expression reads

$$\begin{aligned}
\mathbb{S}_D = & \frac{1}{2} M (\mathbb{D}\mathbf{x}_+)^T \mathbb{H} (\mathbb{D}\mathbf{x}_-) + \frac{1}{2} M (\mathbb{D}\mathbf{y}_+)^T \mathbb{H} (\mathbb{D}\mathbf{y}_-) + \frac{1}{2} I_D (\mathbb{D}\boldsymbol{\theta}_+)^T \mathbb{H} (\mathbb{D}\boldsymbol{\theta}_-) + \frac{1}{2} I_S (\mathbb{D}\boldsymbol{\phi}_+)^T \mathbb{H} (\mathbb{D}\boldsymbol{\phi}_-) + M g \sin(\alpha) \mathbf{1}^T \mathbb{H} \mathbf{x}_- \\
& + \kappa_x (\mathbf{x}_+[1] - x_i) + \tilde{\kappa}_x ((\mathbb{D}\mathbf{x}_-)[1] - \dot{x}_i) + \xi_x (\mathbf{x}_-[N]) + \tilde{\xi}_x (\mathbf{x}_-[N]) \\
& + \kappa_y (\mathbf{y}_+[1] - y_i) + \tilde{\kappa}_y ((\mathbb{D}\mathbf{y}_-)[1] - \dot{y}_i) + \xi_y (\mathbf{y}_-[N]) + \tilde{\xi}_y (\mathbf{y}_-[N]) \\
& + \kappa_\theta (\boldsymbol{\theta}_+[1] - \theta_i) + \tilde{\kappa}_\theta ((\mathbb{D}\boldsymbol{\theta}_-)[1] - \dot{\theta}_i) + \xi_\theta (\boldsymbol{\theta}_-[N]) + \tilde{\xi}_\theta (\boldsymbol{\theta}_-[N]) \\
& + \kappa_\phi (\boldsymbol{\phi}_+[1] - \phi_i) + \tilde{\kappa}_\phi ((\mathbb{D}\boldsymbol{\phi}_-)[1] - \dot{\phi}_i) + \xi_\phi (\boldsymbol{\phi}_-[N]) + \tilde{\xi}_\phi (\boldsymbol{\phi}_-[N]) \\
& + \boldsymbol{\lambda}_-^{\text{D1}} \circ \left((\mathbb{D}\mathbf{x}_+)^T \mathbb{H} (\mathbb{D}\mathbf{x}_+) + (\mathbb{D}\mathbf{y}_+)^T \mathbb{H} (\mathbb{D}\mathbf{y}_+) - R^2 (\mathbb{D}\boldsymbol{\theta}_+)^T \mathbb{H} (\mathbb{D}\boldsymbol{\theta}_+) \right) \\
& - \boldsymbol{\lambda}_+^{\text{D1}} \circ \left((\mathbb{D}\mathbf{x}_+)^T \mathbb{H} \mathbf{x}_- + (\mathbb{D}\mathbf{y}_+)^T \mathbb{H} \mathbf{y}_- - R^2 (\mathbb{D}\boldsymbol{\theta}_+)^T \mathbb{H} \boldsymbol{\theta}_- \right) \\
& + \boldsymbol{\lambda}_-^{\text{D2}} \circ \left((\mathbb{D}\mathbf{x}_+)^T \mathbb{H} \sin[\boldsymbol{\phi}] + (\mathbb{D}\mathbf{y}_+)^T \mathbb{H} \cos[\boldsymbol{\phi}] \right) - (\boldsymbol{\lambda}_+^{\text{D2}})^T \left(\mathbb{H} \sin[\boldsymbol{\phi}] + \mathbb{H} \cos[\boldsymbol{\phi}] \right) \\
& + \kappa_{\lambda^{\text{D1}}} (\boldsymbol{\lambda}_-^{\text{D1}}[1]) + \xi_{\lambda^{\text{D1}}} (\boldsymbol{\lambda}_-^{\text{D1}}[N]) + \kappa_{\lambda^{\text{D2}}} (\boldsymbol{\lambda}_-^{\text{D2}}[1]) + \xi_{\lambda^{\text{D2}}} (\boldsymbol{\lambda}_-^{\text{D2}}[N])
\end{aligned} \tag{A1}$$

⁴ Initial data provides appropriate regularization of the SBP operators as described in detail in [29]

The symbol \circ refers to element-wise multiplication with the array to the right. Since $\boldsymbol{\lambda}_-^{\text{D1}}$ and $\boldsymbol{\lambda}_-^{\text{D2}}$ appear in

combination with derivative terms we need to set them zero at initial and final time via Lagrange multipliers in the last line to avoid unphysical boundary contributions.

2. Discretized action for the particle in a tumbler

Here too physical degrees of freedom are represented on a time grid with N steps $\Delta t = (t_f - t_i)/(N - 1)$ by N -component arrays $\mathbf{x}_{1,2}$, $\mathbf{y}_{1,2}$. Deploying the same SBP discretization described in appendix A 1, adding appropriate Lagrange multipliers to fix the initial and connecting conditions, we obtain the following expression for the discretized action

$$\begin{aligned} \mathbb{S}_S = & \frac{1}{2}M(\mathbb{D}\mathbf{x}_+)^T \mathbb{H}(\mathbb{D}\mathbf{x}_-) + \frac{1}{2}M(\mathbb{D}\mathbf{y}_+)^T \mathbb{H}(\mathbb{D}\mathbf{y}_-) - Mg\mathbf{1}^T \mathbb{H}\mathbf{y}_- \\ & - \frac{V_0}{\sqrt{2\pi\sigma^2}} \left(\exp \left[-((\mathbf{y}_+)^2 + (\mathbf{x}_+)^2 - 1)^2 / (2\sigma^2) \right] \right)^T \mathbb{H}(\mathbf{x}_- \circ \mathbf{x}_+ + \mathbf{y}_- \circ \mathbf{y}_+) \\ & + \kappa_x(\mathbf{x}_+[1] - x_i) + \tilde{\kappa}_x((\mathbb{D}\mathbf{x}_-)[1] - \dot{x}_i) + \xi_x(\mathbf{x}_-[N]) + \tilde{\xi}_x((\mathbb{D}\mathbf{x}_-)[N]) \\ & + \kappa_y(\mathbf{y}_+[1] - y_i) + \tilde{\kappa}_y((\mathbb{D}\mathbf{y}_-)[1] - \dot{y}_i) + \xi_y(\mathbf{y}_-[N]) + \tilde{\xi}_y((\mathbb{D}\mathbf{y}_-)[N]) \end{aligned} \quad (\text{A2})$$

Note that raising a discrete array to a power, as well as applying the exponential function acts element-wise in the above expression.

ing derivatives by finite difference operators \mathbb{D}

$$\begin{aligned} \mathbf{E} = & \\ & \frac{1}{2}M(\mathbb{D}\mathbf{x}_+) \circ (\mathbb{D}\mathbf{x}_+) + \frac{1}{2}M(\mathbb{D}\mathbf{y}_+) \circ (\mathbb{D}\mathbf{y}_+) + Mg\mathbf{y}_+ \end{aligned} \quad (\text{A3})$$

3. Discretized action for the particle sliding on an incline

Again physical degrees of freedom are represented on a time grid with N steps $\Delta t = (t_f - t_i)/(N - 1)$ by N -component arrays $\mathbf{x}_{1,2}$, $\mathbf{y}_{1,2}$. Deploying the same SBP discretization described in appendix A 1 and appendix A 2, adding appropriate Lagrange multipliers to fix the initial and connecting conditions, we obtain the following expression for the discretized action

Due to the use of a mimetic SBP discretization scheme, the discretized mechanical energy \mathbf{E} along time is obtained from the continuum expression simply by replac-

$$\begin{aligned} \mathbb{S}_{\text{SF}} = & \frac{1}{2}M(\mathbb{D}\mathbf{x}_+)^T \mathbb{H}(\mathbb{D}\mathbf{x}_-) + \frac{1}{2}M(\mathbb{D}\mathbf{y}_+)^T \mathbb{H}(\mathbb{D}\mathbf{y}_-) - Mg\mathbf{1}^T \mathbb{H}\mathbf{y}_- \\ & - \frac{V_0}{\sqrt{2\pi\sigma^2}} \left(\exp \left[-(\tan[\alpha]\mathbf{x}_+ - \mathbf{y}_+)^2 / (2\sigma^2) \right] \right)^T \mathbb{H}(\tan[\alpha]\mathbf{x}_- - \mathbf{y}_-) \\ & + \mu \frac{V_0}{\sqrt{2\pi\sigma^2}} \left(\exp \left[-(\tan[\alpha]\mathbf{x}_+ - \mathbf{y}_+)^2 / (2\sigma^2) \right] \right)^T \mathbb{H}(\mathbf{x}_- + \tan[\alpha]\mathbf{y}_-) \\ & + \kappa_x(\mathbf{x}_+[1] - x_i) + \tilde{\kappa}_x((\mathbb{D}\mathbf{x}_-)[1] - \dot{x}_i) + \xi_x(\mathbf{x}_-[N]) + \tilde{\xi}_x((\mathbb{D}\mathbf{x}_-)[N]) \\ & + \kappa_y(\mathbf{y}_+[1] - y_i) + \tilde{\kappa}_y((\mathbb{D}\mathbf{y}_-)[1] - \dot{y}_i) + \xi_y(\mathbf{y}_-[N]) + \tilde{\xi}_y((\mathbb{D}\mathbf{y}_-)[N]) \end{aligned} \quad (\text{A4})$$

As before, raising a discrete array to a power, as well as

applying the exponential function acts element-wise in the above expression.